ELSEVIER

Journal of Chromatography B, 708 (1998) 1–20

JOURNAL OF CHROMATOGRAPHY B

Modified cyclodextrins as chiral selectors: molecular modelling investigations on the enantioselective binding properties of heptakis(2,3-di-O-methyl-6-O-*tert*.-butyldimethylsilyl)-β-cyclodextrin

Thomas Beier[a], Hans-Dieter Höltje[b,*]

[a]*Institute of Pharmacy, Free University of Berlin, Königin-Luise-Str. 2+4, D-14195 Berlin, Germany*
[b]*Institute of Pharmaceutical Chemistry, Heinrich-Heine-University, Universitätsstr. 1, D-40225 Düsseldorf, Germany*

Received 27 May 1997; received in revised form 9 December 1997; accepted 9 December 1997

Abstract

Molecular modelling methods have been used to investigate the enantioselective binding properties of chiral dihydrofuranones on heptakis(2,3-di-O-methyl-6-O-*tert*.-butyldimethylsilyl)-β-cyclodextrin in capillary gas chromatography. A conformational analysis of the modified β-cyclodextrin was performed using annealed molecular dynamics. With the program GRID the molecular interaction potential for each of the received energetically reasonable structures of the β-cyclodextrin and the dihydrofuranones was evaluated using different probe groups. The results of these computations have been used as starting points for constructing geometrically reasonable host–guest complexes between the β-cyclodextrin and the dihydrofuranones. The subsequently performed molecular dynamics simulations yielded different complex states reflecting the conformational flexibility of the diastereomeric complexes. Considering the evaluated interaction energy between the β-cyclodextrin and the dihydrofuranones as a measure of complex stability the results are in close agreement with the experimentally determined elution sequences. The methodology for the construction of the interaction model used in this study is capable of simulating the experimental data. We believe that it may serve as a basis for predictions of hitherto unknown elution sequences at modified cyclodextrins. © 1998 Elsevier Science B.V.

Keywords: Molecular modelling; Enantioselective binding; Cyclodextrins

1. Introduction

Naturally occurring cyclodextrins are cyclic oligomers consisting of six, seven or eight α-(1,4) linked D-glucopyranose units, which are referred to as α-, β- or γ-cyclodextrins, respectively (see Fig. 1). The enzymatic degradation of starch by cyclodextrin glycosyl transferases generally yields a mixture of these three types of cyclodextrins [1,2].

Due to their macrocyclic, conical structure, they are able to form inclusion complexes with a great variety of guest molecules. In the complexed state the included guest molecules frequently exhibit differences in their physico–chemical behavior. Therefore the inclusion property of cyclodextrins has been employed to alter, for example, the aqueous solubility, the bioavailability or the stability of drug molecules [3–7]. Because of the chiral character of the glucose units chiral guest molecules can form diastereomeric complexes with cyclodextrins. This

*Corresponding author.

0378-4347/98/$19.00
PII S0378-4347(97)00636-1

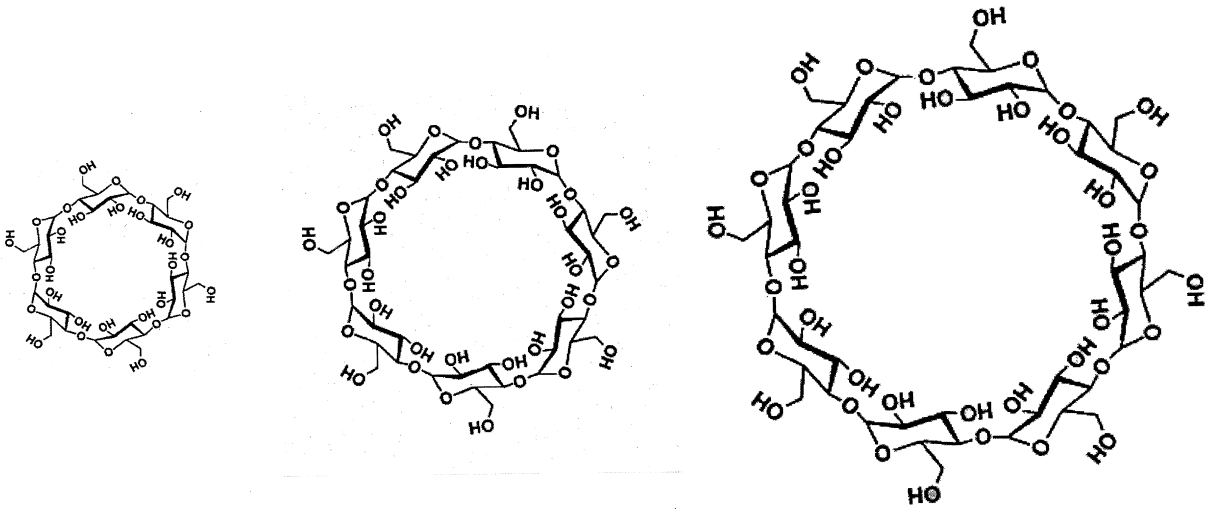

Fig. 1. Schematic representation of α-, β- and γ-cyclodextrin.

property offers the possibility to utilize cyclodextrins in the enantioselective analysis. Especially chromatographic methods with the reversible diastereomeric association between solute and selectand allows the chiral discrimination of a wide range of compounds [8–12].

The different physico–chemical requirements of the chromatographic methods encouraged the development of various modified cyclodextrins used as stationary phases in the enantioselective separation of chiral compounds [13]. Preferred variations in the substitution pattern have been the alkylation or acylation of the hydroxyl groups in position C2, C3 and C6 [14–18] (for atom numbering see Fig. 2). In particular modified cyclodextrins diluted with polysiloxanes have become powerful tools in the enantioselective capillary gas chromatography. One very recent and successful application is the enantioselective analysis of aroma-relevant dihydrofuranones in the authenticity control of flavors and fragrances [19].

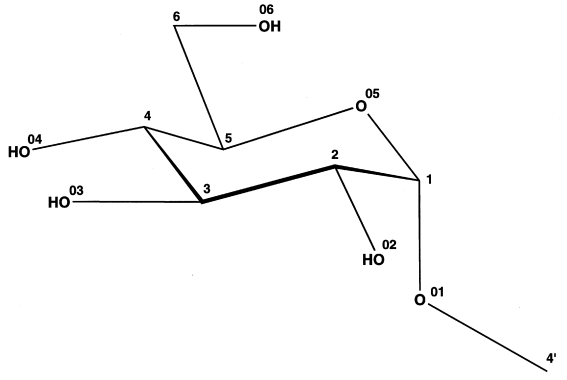

Fig. 2. Atom numbering of α-D-methylglucose.

The use of the modified cyclodextrin heptakis(2,3-di-O-methyl-6-O-*tert.*-butyldimethylsilyl)-β-cyclodextrin allows the chiral resolution of α,β unsaturated γ-lactones (Fig. 3).

These furanone derivatives are well known flavor compounds. Because of their high odor activity, they are interesting substances for studying structural relationships between chirality and odor impression. In addition, due to the experimentally obtained separation factors the data seem to be especially suitable for molecular modelling investigations.

The description of the different binding of the optical antipodes in the chromatographic separation process by molecular modelling methods is a difficult task. As the molecular descriptors are the same the enantiomers are in principle able to make the same kind of interaction with the stationary phase. Therefore a differentiation is only possible by precisely quantifying the intermolecular binding energy between solute and cyclodextrin. The separation factor α is related to the differential free energy of binding of the *R*- and *S*-enantiomers by $\Delta_{R/S}\Delta G = -R \cdot T \ln \alpha$. Because of the small free energy differ-

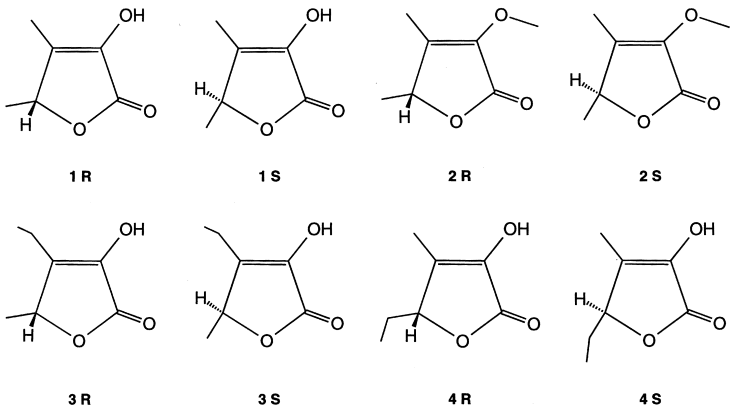

Fig. 3. The investigated dihydrofuranones: (**1**) (*R*/*S*)-4,5-dimethyl-3-hydroxy-2[5*H*]-furanone; (**2**) (*R*/*S*)-4,5-dimethyl-3-methoxy-2[5*H*]-furanone; (**3**): (*R*/*S*)-4-ethyl-3-hydroxy-5-methyl-2[5*H*]-furanone; (**4**) (*R*/*S*)-5-ethyl-3-hydroxy-4-methyl-2[5*H*]-furanone.

ences corresponding to the observed α values the experimental data should reflect high enantioselectivity of the stationary phase.

Since the responsible forces for the separation of the enantiomers are still unknown in detail it is of particular interest to get insight into the mechanism of the separation process. The aim of our molecular modelling study is to construct a corresponding interaction model of the host–guest complexes in order to be able to describe the forces which are responsible for the enantiomeric separation. Further on, the correct elution order of the separated optical antipodes can only be assigned by coinjection of optically pure reference substances. Since information about the absolute configuration of the separated enantiomers or reference substances are not available in some cases, the constructed interaction model has been used as a basis for the prediction of hitherto unknown elution sequences of the enantiomers of the compounds **3** and **4**.

2. Methods

The molecular graphics studies and the molecular dynamics simulations were carried out on SILICON GRAPHICS INDIGO workstations and on a SILICON GRAPHICS POWER CHALLENGE using BIOSYM software INSIGHT/DISCOVER [20]. On the basis of ab initio calculations [21] and experimental data the CVFF force field of INSIGHT/DISCOVER has been adjusted so that the special geometrical properties of carbohydrates are more correctly reflected. It is well known that these properties at the anomeric carbon atom are caused by the anomeric effect [22]. To take account for this phenomenon in molecular mechanics calculations special parameters have to be added to the force field [23].

In a recent study it has been shown that the conformational behavior of oligosaccharides is well predicted by the CVFF force field [24]. As β-cyclodextrins are composed of seven α-(1,4) linked D-glucose units we have chosen α-D-methylglucose as a model compound (see Fig. 2) to test the ability of CVFF force field calculations to fit the bond length variation in the anomeric C–O–C–O–C atomic sequence. In the first step the structure has been relaxed performing an ab initio calculation using the 6-31G* basis set and complete geometry optimization. The results of these computations have been compared with CVFF force field calculations and experimental data [25]. The CVFF force field parameters for the bonds next to the anomeric carbon atom had to be adjusted in order to show good agreement with the ab initio and experimental data (see Fig. 4). The modified bond length and bond angle parameters used in the subsequent calculations are given in Table 1.

The molecular structure of the heptakis(2,3-di-O-methyl-6-O-*tert*.-butyldimethylsilyl)-β-cyclodextrin was derived from the crystal structure of β-cyclo-

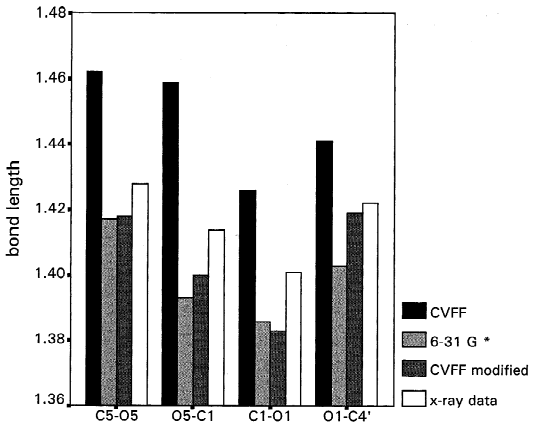

Fig. 4. Comparison of the bond lengths in Å next to the anomeric carbon; for atom numbering see Fig. 2.

dextrin [26] taking the molecular coordinates from the Cambridge Crystallographic Database [27] and modifying the substituents using the builder module within INSIGHT II. For the dihydrofuranone derivatives the five membered ring systems have been initially taken from the standard fragment library of INSIGHT II and subsequently the substituents added applying the same procedure as for the β-cyclodextrin.

With regard to the dynamical process in chromatographic resolution the most realistic picture of the cyclodextrin molecule will not be reflected by the single crystal structure of the modified cyclodextrin but by considering also the mobility of the macrocycle. In order to investigate this conformational flexibility of the host molecule a comprehensive conformational analysis of the heptakis(2,3-di-O-methyl-6-O-*tert.*-butyldimethylsilyl)-β-cyclodextrin has been performed. For this purpose we carried out high temperature annealed molecular dynamics simulations starting at 1000 K annealing to 0 K. The efficiency and suitability of the simulated annealing method in conformational analysis of highly flexible and complex molecules has been shown in several successful applications [28–31]. The temperature of 1000 K is necessary to enable the molecule to overcome energy barriers between different conformations and to prevent the system from getting stuck in a particular region of conformational space. Simulations at lower temperatures yielded very similar conformations while higher temperatures led to distorted geometries.

At the beginning of the simulation protocol the heptakis(2,3-di-O-methyl-6-O-*tert.*-butyldimethylsilyl)-β-cyclodextrin was relaxed using the steepest descent method for 100 steps until a derivative of 1.0 kcal mol^{-1} was reached. After the relaxation of the modified β-cyclodextrin the molecular dynamics simulation was initialized using a time step of 1 fs. The equilibrium time was selected to be 20 ps before data collection started and all atoms were allowed to move without applying the SHAKE algorithm [32]. The temperature was held constant by coupling the system to a temperature bath yielding a canonical ensemble as provided by default in the DISCOVER program.

In regular time intervals of 30 ps the system cooled down by decreasing the temperature to 0 K. Applying this procedure the molecule is trapped in a local minimum conformation resulting in an energetically reasonable geometry. The conformation obtained at the end of the annealing cycle was saved and subsequently used as a starting point for the next cycle. With the objective to generate a pool of different minimum energy structures, conformations at the end of 30 annealing cycles have been collected.

Crystal data and NMR measurements show the glucose units in cyclodextrins to adopt the energetically favorable $^4C_1$ chair conformation. For this reason cyclodextrin molecules with boat, skew-boat

Table 1
Modified force field parameters for the anomeric atomic sequence

	Bond length parameter	Force constant		Bond angle parameter	Force constant
C5–O5	1.370	273.2	C5–O5–C1	109.5	60.0
O5–C1	1.350	273.2	O5–C1–O1	109.5	70.0
C1–O1	1.350	273.2	C1–O1–C4′	109.5	60.0
O1–C4′	1.400	273.2	C2–C1–O5	109.5	70.0

or half-chair glucose conformations have been rejected as high temperature simulation artefacts yielding a total of 22 energetically reasonable conformations of heptakis(2,3-di-O-methyl-6-O-*tert.*-butyldimethylsilyl)-β-cyclodextrin. The conformational space of the dihydrofuranone derivatives was investigated following the same scheme.

The results of the molecular dynamics simulation demonstrate the high conformational flexibility of the heptakis(2,3-di-O-methyl-6-O-*tert.*-butyldimethylsilyl)-β-cyclodextrin. In some of the sampled low energy conformations the annular shape of the starting structure (see Fig. 5) has nearly been preserved while in other geometries the cavity has collapsed. As a consequence of the bulky substituent at position C6 of the glucose units the narrow opening of the cyclodextrin is partially blocked. However, in spite of the methoxy substituents at the C2 and C3 position at the wider opening there remains enough space for ligands to enter the cavity (see Fig. 6).

The conformational flexibility of alkylated cyclodextrins in vacuo simulations has also been observed in solution. Because of the large number of hydroxyl groups in native β-cyclodextrins a tight network of inter- and intramolecular hydrogen bonds is formed [33–36]. Due to this property these molecules adopt a symmetrical and rigid geometry. On account of the complete substitution of the hydroxyl groups this kind of interaction is lost. The flexibility of the heptakis(2,3-di-O-methyl-6-O-*tert.*-butyldimethylsilyl)-β-cyclodextrin demonstrated in the molecular dynamics simulation therefore represents a realistic picture of the conformational properties of this structure.

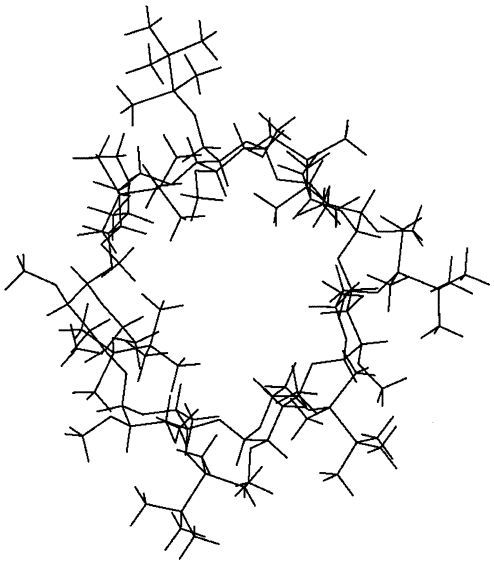

Fig. 5. Starting structure for the conformational analysis of heptakis(2,3-di-O-methyl-6-O-*tert.*-butyldimethylsilyl)-β-cyclodextrin deduced from the crystal structure of β-cyclodextrin [26].

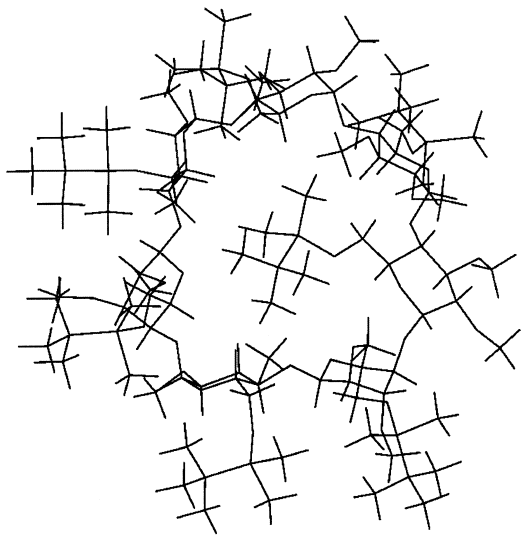

Fig. 6. One of the minimum energy conformations obtained by annealed molecular dynamics.

The initial step in diastereomeric complex formation is the recognition event. Due to the long range effects of electrostatic forces, recognition occurs at rather large distances and precedes the formation of the final cyclodextrin–ligand complex. The three-dimensional electrostatic field surrounding each molecule therefore plays a crucial role in recognition. To properly measure the electrostatic properties of both ligand and cyclodextrin the partial charges have been taken from ab initio calculations using the 6-31G* basis set [37]. In comparison with the two semiempirical methods AM1 and PM3 [38–41] calculated dipole moments of several rigid test compounds revealed the ab initio procedure to be the most suitable method for the planned investigations. Therefore atomic charges have been derived from the quantum mechanically calculated wavefunctions (6-

31G* basis set) by using the electrostatic potential fit method (ESP-method) [42,43].

Owing to the size of the modified cyclodextrin the calculation of the wavefunction was not feasible for the entire molecule. We have evaded this impediment by dividing the cyclodextrin into fragments. As the heptakis(2,3-di-O-methyl-6-O-*tert.*-butyldimethylsilyl)-β-cyclodextrin is composed of seven equivalent glucose units one glucose molecule was taken as representative for the whole cyclodextrin molecule. Wavefunctions and partial charges were calculated for this fragment and the results then have been transfered onto the whole cyclodextrin molecule.

The approaching ligand molecule endeavors to locate regions of attraction necessary for specific and tight binding. Due to the multitude of possible interaction points in the cyclodextrin it is nearly impossible to detect an energetically reasonable geometry for the host–guest interaction by using a simple docking procedure.

In order to model the potential host–guest interactions as closely as possible, the molecular interaction potential (MIP) for the heptakis(2,3-di-O-methyl-6-O-*tert.*-butyldimethylsilyl)-β-cyclodextrin as well as for the dihydrofuranone derivatives was evaluated using the program GRID [44]. Program GRID is an approach to predict noncovalent interactions between a target molecule and a chemical probe group moved around the target in a three-dimensional grid. The probe groups reflect chemical characteristics of the corresponding binding partner or fragments of it.

Chromatographical separation processes are characterized by the reversible binding between the stationary phase and the solute. During separation the enantiomers will form intermediate diastereomeric complexes of various stabilities and life times with the chiral selector. The differences in complex stabilities determine the retention times of the optical antipodes and thus the chiral discrimination. The most realistic simulation of this reversible process can therefore not be obtained by consideration of a single diastereomeric complex but by analysis of a variety of diastereomeric complex geometries. For this reason the MIPs for all the low energy conformations of the host molecules were evaluated using a methyl probe and a hydroxyl probe. Correspondingly, for the guest molecules MIPs with a methyl probe and an ether oxygen probe have been computed. Using these particular probe groups it should be possible to precisely locate favorable binding regions for van der Waals interactions as well as potential binding geometries leading to hydrogen bond formation. The molecular interaction fields obtained from the GRID computations indicate favorable positions where the functional groups of the ligand molecules should preferentially bind to the host molecule.

The GRID calculations detected the most preferred regions for attraction between the heptakis(2,3-di-O-methyl-6-O-*tert.*-butyldimethylsilyl)-β-cyclodextrin and the methyl probe at the wider rim and in the cavity of the cyclodextrin (see Fig. 7). This is due to the orientations of the methoxy substituents in position C2 and C3 of the glucose units. Using an aliphatic hydroxyl group the interaction fields indicate binding sites for a potential hydrogen bond donator. Although all ether oxygen atoms in the cyclodextrin in principle are capable of accepting a hydrogen bond, only some of them in each considered cyclodextrin conformation are in an optimal orientation in the represented conformation to form a stable hydrogen bond interaction.

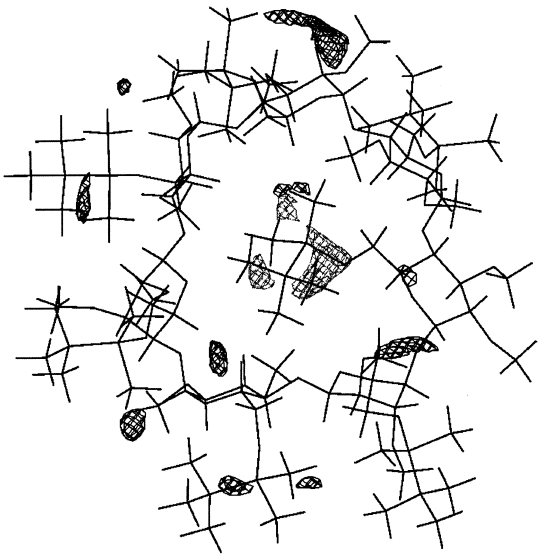

Fig. 7. The regions of attraction between the heptakis(2,3-di-O-methyl-6-O-*tert.*-butyldimethylsilyl)-β-cyclodextrin and the probe groups. The GRID spaces are contoured at −3.5 kcal/mol for the hydroxyl group (black) and at −3.0 kcal/mol for the methyl group (grey).

The MIPs of the dihydrofuranones clearly show the overall affinities of the investigated ligands to the host molecule. The distinct substitution patterns of the ligands cause interaction fields of different size and orientation obtained with the methyl probe (see Fig. 8). For the ethyl substituted congeners of the series the corresponding GRID fields are more extended compared to the analogues **1** and **2**. In the case of the 4,5-dimethyl-3-methoxy-2[5*H*]-furanone **2R** and **2S** this is the only kind of interaction possibility with the cyclodextrin. As a consequence of the methoxy substitution the ability to form hydrogen bonds has been lost.

GRID contours calculated by using an ether oxygen probe label favorable hydrogen bond regions. Because of sterical hindrance the interactions between the probe and the hydroxyl substituents of the ligands **3R** and **4R** are not as strong as for the analogue **1R**. For this reason the GRID fields are contoured at −2.5 kcal/mol for compound **1R** and at −2.0 and −2.2 kcal/mol for compounds **3R** and **4R**, respectively. The described molecular interaction fields have been subsequently utilized as a matrix in the construction of the host–guest complex geometries.

Several attempts have been made in earlier studies to solve the docking problem of the ligand into the cyclodextrin [45–48]. It has been recognized that the positioning of the guest molecule deep into the cavity is somewhat arbitrary and the generation of reasonable complex geometries has to be performed more carefully. In our docking procedure we employed the GRID fields in combination with steric parameters reflecting the steric demands of both ligands and the cyclodextrin.

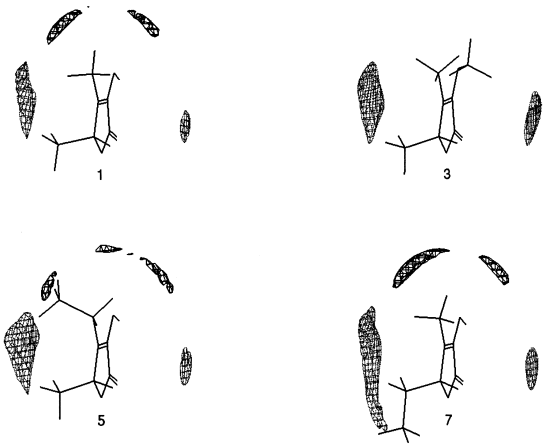

Fig. 8. GRID contours of the dihydrofuranones **1R** (1), **2R** (3), **3R** (5) and **4R** (7) using a methyl group (grey) contoured at −1.2 kcal/mol and an ether oxygen probe (black) contoured at −2.5 kcal/mol for compound **1** and at −2.0 and −2.2 kcal/mol for compounds **3** and **4**, respectively.

The developed interaction model is based on the assumption that ligand and cyclodextrin form 1:1 complexes. Contrary to the observation of some 2:1 complexes in crystals [49] the situation in solution is different. In contrast to the tight packing in the crystal environment the dilution effect prevents a close approximation of cyclodextrin molecules especially at high temperatures applied in gas chromatography. Comprehensive X-ray studies [50–53] and NMR investigations [54–56] of cyclodextrin inclusion compounds indicate the preferred binding site for small guest molecules at the wider rim or at the opening of the cyclodextrin cavity. This is of particular interest in the chiral recognition process because the chiral centers at C2 and C3 of the corresponding glucose units were discussed to be of special importance [57,58].

Therefore, whenever possible, during the docking process of the ligand above all those regions of the MIPs have been utilized, where the guest molecule can be placed at the wider opening of the cyclodextrin cavity. For the docking the corresponding module of the software package INSIGHT II was used. The automatically obtained complex geometries subsequently were manually altered in order to include the GRID interaction fields. The resulting positions for the enantiomers were chosen to be the same for the *R*- and the *S*-form in order to provide for both the same conditions at the starting point.

As an example the starting geometry of one of the interaction complexes between (*R*)-4,5-dimethyl-3-hydroxy-2[5*H*]-furanone and the heptakis(2,3-di-O-methyl-6-O-*tert*.-butyldimethylsilyl)-β-cyclodextrin is given in Fig. 9.

On the basis of the MIPs the docking procedure yields energetically attractive interaction geometries for the host–guest complex. In the complex geometry presented in Fig. 9 an attractive interaction with the ring system of the (*R*)-4,5-dimethyl-3-hydroxy-2[5*H*]-furanone is offered to a methoxy group of the cyclodextrin. A supplementary stabilization of this

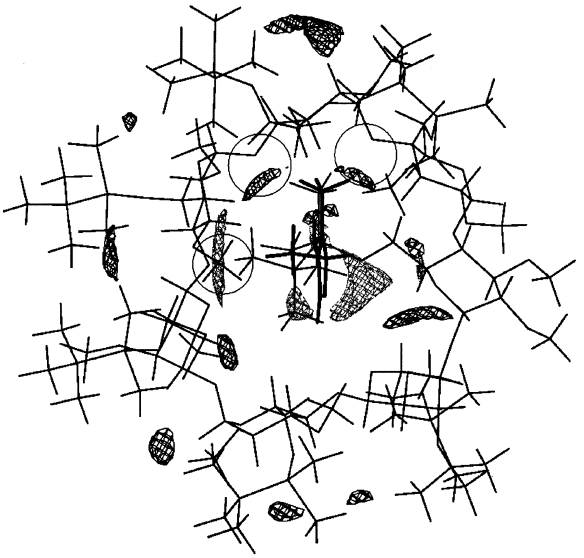

Fig. 9. Host–guest complex between heptakis(2,3-di-O-methyl-6-O-*tert.*-butyldimethylsilyl)-β-cyclodextrin and (*R*)-4,5-dimethyl-3-hydroxy-2[5*H*]-furanone **1**. The atoms and groups involved in the possible host–guest interaction are marked with a circle.

interaction geometry is provided by hydrogen bonds between the hydroxyl group of (*R*)-4,5-dimethyl-3-hydroxy-2[5*H*]-furanone and glycosidic ether oxygen atoms of the cyclodextrin. In the case of the methoxy analogues (compounds **2R** and **2S**) of the 4,5-dimethyl-3-hydroxy-2[5*H*]-furanone only van der Waals forces can contribute to the stabilization of the interaction complexes.

In order to investigate the flexibility of the obtained host–guest geometries molecular dynamics (MD) calculations have been performed. In recent years MD calculations have become powerful tools in molecular modelling studies. By means of MD the time-dependent motional behavior of a molecular system can be reproduced. The calculated trajectory allows the evaluation of several properties of the molecular system over the simulation period.

During the MD simulation the host–guest complexes were able to change conformation in order to reach closer contacts between the embedded guest molecule and the cyclodextrin. The capability to be subjected to an induced-fit like mechanism is an essential contribution to the chiral recognition process while the loss of flexibility in more rigid cyclodextrin congeners leads to a drastic decrease in enantioselectivity [59].

Before discussing the results of the MD simulations some basic assumptions made in the presented interaction model have to be explained. Since the heptakis(2,3-di-O-methyl-6-O-*tert.*-butyldimethylsilyl)-β-cyclodextrin is dissolved in the polysiloxane PS 268 (polydimethyl-diphenyl-methyl-vinylsiloxane) the solvent environment has to be regarded. Comprehensive investigations on the importance of different polysiloxanes used in column preparation revealed the influence of the employed solvent on the separation quality [60–63]. The only practicable way to represent the solvent effects in MD simulations however is to take into account the corresponding dielectric constant. The contribution of solvent molecules to the separation process is of achiral nature. Both enantiomers experience the same type of interactions. Therefore the complex mechanism of chiral recognition can be reduced to the interaction between the chiral guest molecules and the cyclodextrin. This approximation is supported by the observation that no enantiomeric separation takes place in the absence of the cyclodextrin.

In the discussion of the solvent influence on the separation quality the polysiloxanes are often classified as polar/moderately polar/apolar. The consideration of solvent effects in theoretical investigations however requires a more detailed description of the polysiloxane properties. As already mentioned the cyclodextrin environment in the calculations is represented by including the solvents dielectric constant. While only little detailed information about the dielectric properties of the interesting polysiloxane was available, the dielectric constant ε was experimentally determined for PS 268 (ε=2.948) and introduced into the electrostatic term of the force field equations in order to represent the solvent effects of the polysiloxane matrix used in column preparation.

As a result of the docking procedure 22 different host–guest geometries for each enantiomer of the compounds **1–4** have been generated. These host–guest complexes have been used as starting points for the subsequent MD simulations. In order to remove the internal strain in the complexes resulting from the docking process the starting geometry of each complex has been subjected to a geometry

optimization. After 50 optimization steps of steepest descent followed by 100 steps using conjugate gradient the host–guest complexes were sufficiently relaxed to serve as input geometry for the MD runs.

To obtain a realistic picture of all forces involved in the binding process, charges have been included and the dielectric constant has been considered to reflect the solvent properties. The simulation temperature has been chosen to be 380 K which corresponds to the average temperature of the gas chromatographic separation process.

In the first step the MD simulation has been initialized at 380 K and after an equilibrium time of 10 ps data collection has been started. The simulation time for every single MD run was selected to be 200 ps and the complex geometries have been saved every 250 simulation steps (250 fs) resulting in 800 different complex states. For each of the recorded states the interaction energy and the hydrogen bonding pattern (except for the compounds **2R** and **2S**) was determined. A prerequisite for a reasonable evaluation of the MD simulations are stable cyclodextrin–ligand complexes during the whole simulation period. For all starting geometries this has been true, modifications of the MD parameters therefore have not been necessary.

The most important criterion for the stability of interaction complexes is the energy of interaction between the ligands and the cyclodextrin host. Interaction energies have been calculated for all 800 complex geometries and the mathematical average of these interaction energy values has been used as a measure of complex stability. A Boltzmann weighted average of the interaction energies would yield a dramatic reduction of the different complex geometries considered. In addition, also the amount of complexes used for the evaluation of the retention power of the cyclodextrin for *R* and *S*-enantiomers could differ. This situation is by no means desirable, because in view of the experimentally detected retention times only small differences in the energies of interaction for *R* and *S*-enantiomers probably decide upon the retention order of the enantiomeric pairs. Since we have not performed a Boltzmann weighting of the interaction energies a statistical procedure had to be applied for comparison of the 22

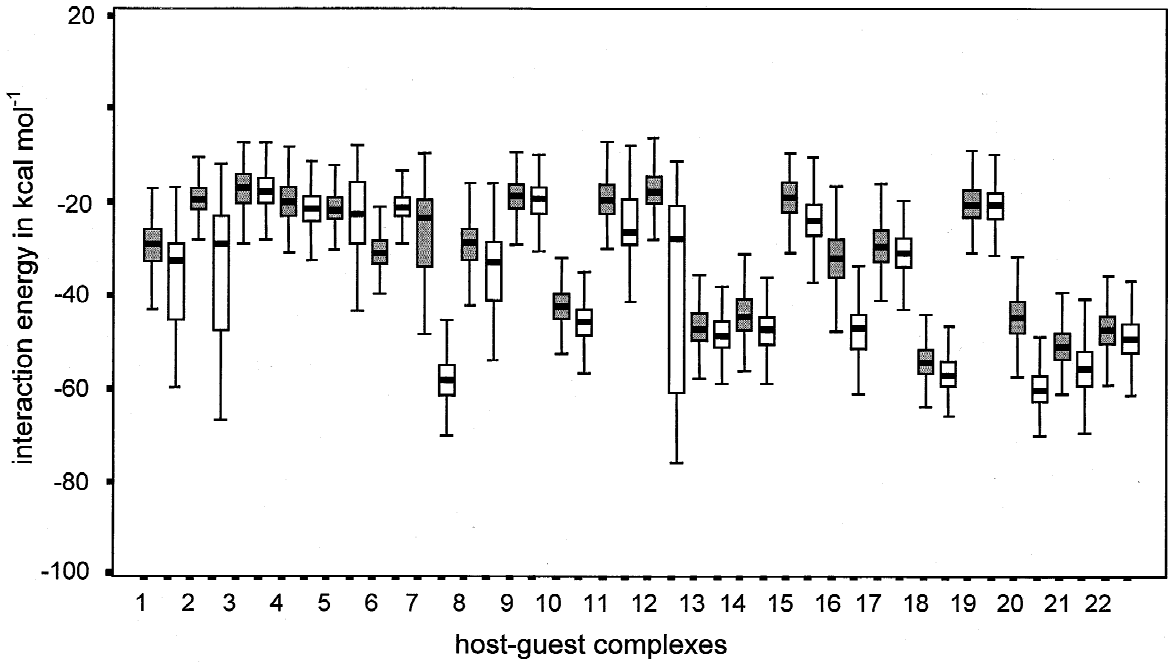

Fig. 10. Box and Whisker plots of the calculated interaction energies for the complexes 1–22 of the compounds **1R** and **1S**. For the *R*-enantiomer the Box and Whisker plots are shown in grey and for the corresponding *S*-enantiomer in white, respectively.

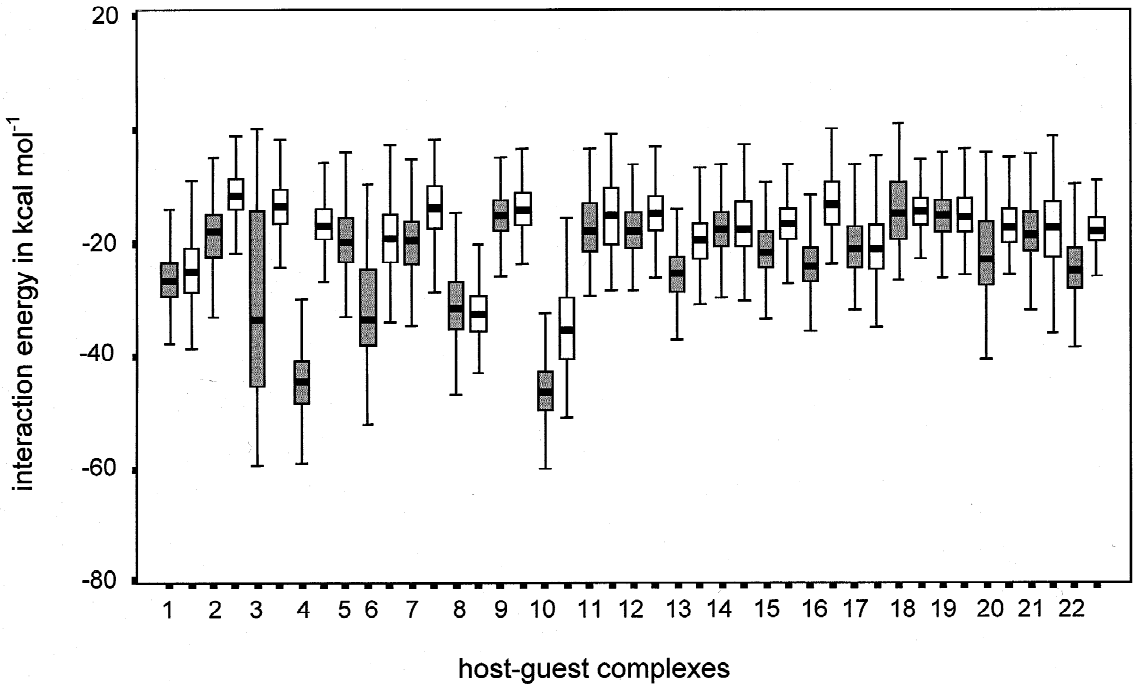

Fig. 11. Box and Whisker plots of the calculated interaction energies for the complexes 1–22 of the compounds **2R** and **2S**. For the *R*-enantiomer the Box and Whisker plots are shown in grey and for the corresponding *S*-enantiomer in white, respectively.

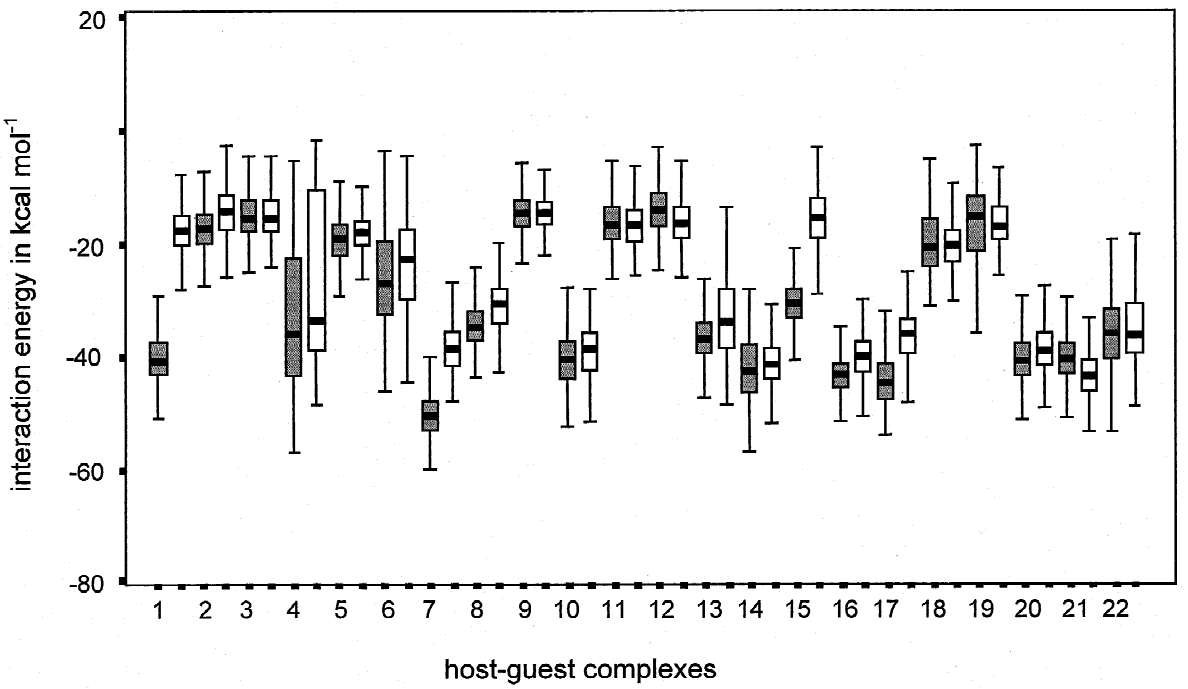

Fig. 12. Box and Whisker plots of the calculated interaction energies for the complexes 1–22 of the compounds **3R** and **3S**. For the *R*-enantiomer the Box and Whisker plots are shown in grey and for the corresponding *S*-enantiomer in white, respectively.

average energies calculated for each of the guest molecules. The statistical method selected is the median test, which must be applied if the data which are to be compared do not possess an equal distribution. If the average energies of interaction are presented in the form of box-and-whisker plots (see Figs. 10–13) it can be easily seen, that this indeed is the case. As a result of the median test it was found that for all four enantiomeric pairs one enantiomer was always significantly preferred over the other with respect to the interaction energies. Although this is not true for all of the single 22 different starting complex geometries the corresponding retention orders could be determined unequivocally.

In addition to the evaluation of the interaction energies and the hydrogen bonding pattern a collection of the energetically most preferred complex states of each MD run has been analyzed in order to detect similarities or diversities in the enantioselective binding behavior of the dihydrofuranones. By means of a close inspection of individual complexes useful hints for the separation mechanism should be deducible.

3. Results

The resulting interaction energies of compounds **1** and **2** significantly correlate with the experimentally determined elution sequences. In these cases the absolute configurations of the separated enantiomeric pairs have been detected by means of X-ray crystallography. The inclusion of the ligands plays an important role in the chiral separation process. For **1R** and **1S** (*R*- and *S*-enantiomers of 4,5-dimethyl-3-hydroxy-2[5*H*]-furanone) the number of hydrogen bonding contacts is nearly identical. The hydrogen bonding partners for **1S**, however, were located deeper in the cavity than for **1R**. Therefore, for ligand **1S** close contacts in the interior of the cyclodextrin cavity are possible yielding more negative interaction energies. The deep embedding in the cavity allows to form hydrophobic contacts between the methyl group attached to the chiral center and the methoxyl groups of the heptakis(2,3-di-O-methyl-6-O-*tert*.-butyldimethylsilyl)-β-cyclodextrin (see Fig. 14). These energetically favorable complex geometries can be further stabilized by hydrogen bonds. All

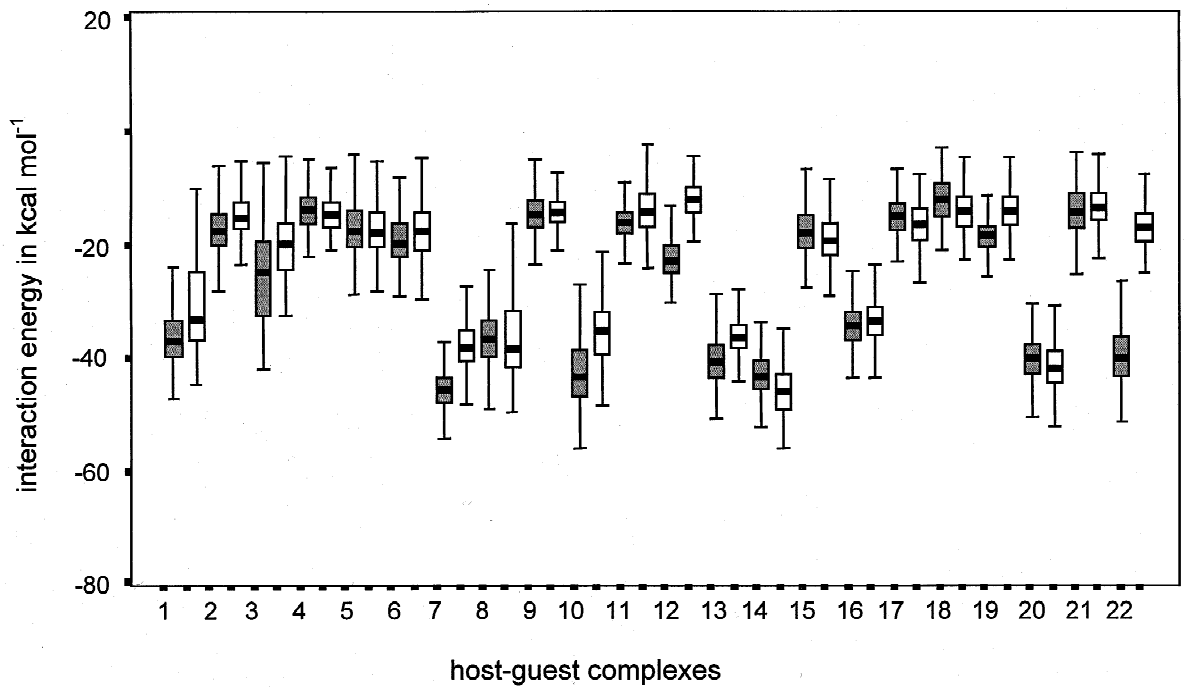

Fig. 13. Box and Whisker plots of the calculated interaction energies for the complexes 1–22 of the compounds **4R** and **4S**. For the *R*-enantiomer the Box and Whisker plots are shown in grey and for the corresponding *S*-enantiomer in white, respectively.

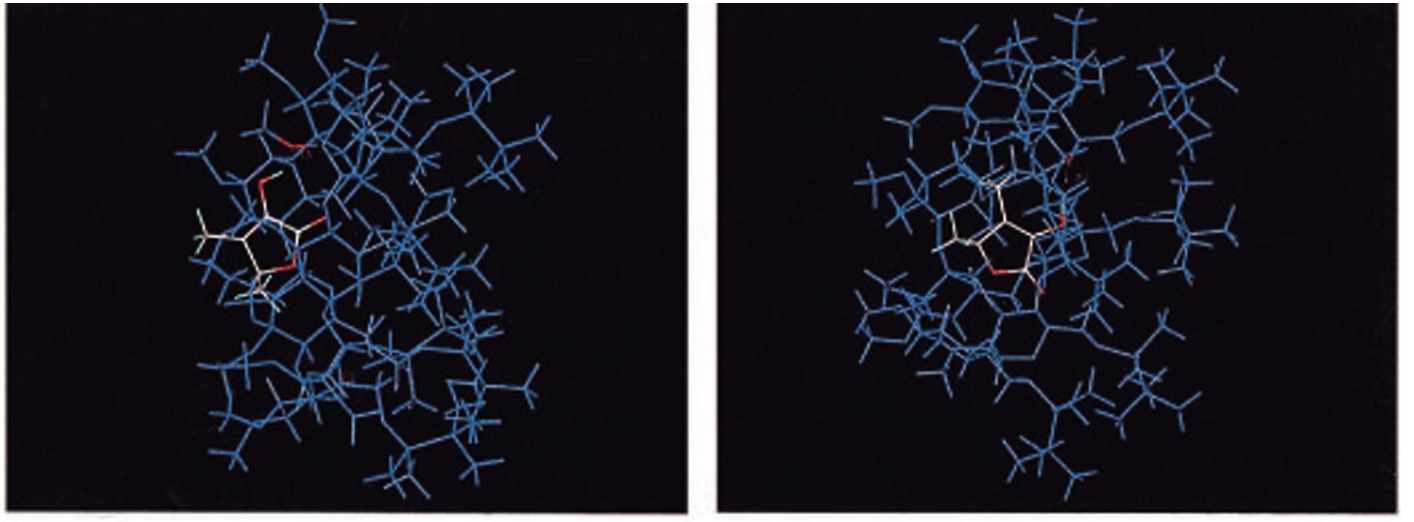

Fig 14.

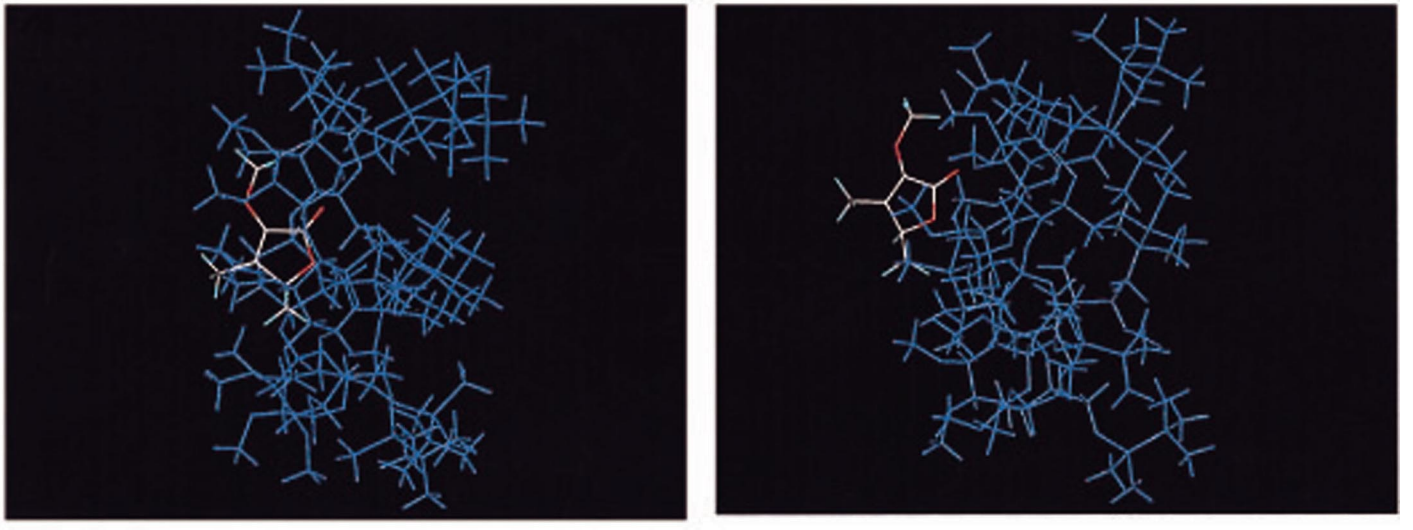

Fig 15.

Fig. 14. One of the favourable complex geometries between **1R** (left side) and **1S** (4,5-dimethyl-3-hydroxy-2[5*H*]-furanone) and heptakis(2,3-di-O-methyl-6-O-*tert*.-butyldimethylsilyl)-β-cyclodextrin. The possible H-bond interaction is marked by dotted lines.

Fig. 15. One of the favourable complex geometries between **2R** (left side) and **2S** (4,5-dimethyl-3-methoxy-2[5*H*]-furanone) and heptakis(2,3-di-O-methyl-6-O-*tert*.-butyldimethylsilyl)-β-cyclodextrin. As a consequence of the sterically more demanding methoxy substituent a deep penetration into the cavity is more difficult.

the described effects contribute collectively to the tighter binding of the *S*-enantiomer. The calculated average energies of interaction are shown in Table 2. In the median test (Fig. 10) the *S*-enantiomer was preferred over the *R*-enantiomer for 20 out of the 22 compared pairs.

For ligands **2R** and **2S** (*R*- and *S*-enantiomers of 4,5-dimethyl-3-methoxy-2[5*H*]-furanone) the situation is somewhat different. The sterically more demanding methoxyl substituent impedes both the *R*- and the *S*-enantiomer to penetrate deeply into the cavity. The locations of **2R** and **2S** during the MD simulations above all are at the wider rim of cyclodextrin (see Fig. 15). The *R*-complexes are more stable than the *S*-complexes in 16 out of the 22 pairs (see Table 3 and Fig. 11). As a consequence of the restricted access to the cavity **2R** and **2S** were not able to form very strong diastereomeric complexes desirable for optimal enantioselectivity. Also, the stabilizing effect of the hydrogen bonds is missing. Therefore the calculated interaction energy differences between the enantiomers was found to be smaller than that found for **1R** and **1S** resulting in a decrease in enantioselectivity. This is fully consistent with chromatographic retention orders and separation data.

The 4-ethyl substituent of **3R** and **3S** (4-ethyl-3-hydroxy-5-methyl-2[5*H*]-furanone) is able to fix the ligands in an orientation of favorable interaction with the inside of the cyclodextrin and to form strong contacts with the chiral centers at the lip of the cyclodextrin cavity. In these stable orientations **3R** and **3S** are mostly involved in hydrogen bonds to the ether oxygen atoms of the cyclodextrin (see Fig. 16). During the MD simulations the *S*-enantiomer experiences more fluctuations in the diastereomeric

Table 2
Median $\tilde{x}$ of the interaction energy with the confidence interval CI$\tilde{x}$ ($\alpha=0.05$) of the compounds **1R** and **1S**

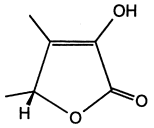

1 R

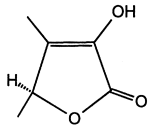

1 S

CD	$\tilde{x}$	CI$\tilde{x}$	$\tilde{x}$	CI$\tilde{x}$
1	−29.532	$-29.877\leq\tilde{x}\leq-29.008$	−34.441	$-35.331\leq\tilde{x}\leq-33.434$
2	−16.798	$-17.118\leq\tilde{x}\leq-16.440$	−29.362	$-31.071\leq\tilde{x}\leq-27.846$
3	−13.237	$-13.790\leq\tilde{x}\leq-12.723$	−14.502	$-14.942\leq\tilde{x}\leq-14.098$
4	−17.653	$-18.240\leq\tilde{x}\leq-17.027$	−19.351	$-19.734\leq\tilde{x}\leq-18.870$
5	−19.760	$-20.055\leq\tilde{x}\leq-19.265$	−20.725	$-21.470\leq\tilde{x}\leq-19.787$
6	−32.155	$-32.623\leq\tilde{x}\leq-31.810$	−19.159	$-19.505\leq\tilde{x}\leq-18.830$
7	−22.101	$-23.298\leq\tilde{x}\leq-21.188$	−68.833	$-69.199\leq\tilde{x}\leq-68.026$
8	−29.211	$-30.027\leq\tilde{x}\leq-28.519$	−34.564	$-35.646\leq\tilde{x}\leq-33.618$
9	−15.557	$-16.061\leq\tilde{x}\leq-15.033$	−16.411	$-16.819\leq\tilde{x}\leq-16.013$
10	−47.388	$-47.833\leq\tilde{x}\leq-46.893$	−52.047	$-52.403\leq\tilde{x}\leq-51.495$
11	−16.836	$-17.352\leq\tilde{x}\leq-16.281$	−26.045	$-26.776\leq\tilde{x}\leq-25.189$
12	−14.491	$-15.183\leq\tilde{x}\leq-13.861$	−27.890	$-29.931\leq\tilde{x}\leq-29.196$
13	−54.108	$-54.552\leq\tilde{x}\leq-53.571$	−55.953	$-56.334\leq\tilde{x}\leq-55.502$
14	−50.363	$-50.990\leq\tilde{x}\leq-49.725$	−54.427	$-55.023\leq\tilde{x}\leq-53.861$
15	−16.127	$-16.524\leq\tilde{x}\leq-15.576$	−22.752	$-23.294\leq\tilde{x}\leq-21.999$
16	−33.748	$-34.322\leq\tilde{x}\leq-33.089$	−53.939	$-54.805\leq\tilde{x}\leq-53.187$
17	−30.160	$-30.672\leq\tilde{x}\leq-29.573$	−32.298	$-32.799\leq\tilde{x}\leq-31.821$
18	−63.753	$-64.172\leq\tilde{x}\leq-63.323$	−67.322	$-67.629\leq\tilde{x}\leq-66.903$
19	−18.204	$-18.688\leq\tilde{x}\leq-17.701$	−18.325	$-18.831\leq\tilde{x}\leq-17.883$
20	−50.782	$-51.484\leq\tilde{x}\leq-50.240$	−71.707	$-72.221\leq\tilde{x}\leq-71.248$
21	−59.262	$-59.798\leq\tilde{x}\leq-58.742$	−65.482	$-66.010\leq\tilde{x}\leq-64.859$
22	−54.400	$-54.876\leq\tilde{x}\leq-53.931$	−56.910	$-57.336\leq\tilde{x}\leq-56.469$

In the first row the numbering of the starting complex is given.

Table 3
Median $\tilde{x}$ of the interaction energy with the confidence interval CI$\tilde{x}$ ($\alpha=0.05$) of the compounds **2R** and **2S**

	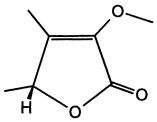 **2 R**		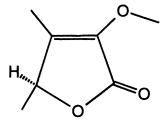 **2 S**	
CD	$\tilde{x}$	CI$\tilde{x}$	$\tilde{x}$	CI$\tilde{x}$
1	−26.472	$-26.847\leq\tilde{x}\leq-25.946$	−24.955	$-25.383\leq\tilde{x}\leq-24.421$
2	−17.752	$-18.025\leq\tilde{x}\leq-17.353$	−11.459	$-11.740\leq\tilde{x}\leq-11.064$
3	−33.389	$-37.462\leq\tilde{x}\leq-28.327$	−13.587	$-13.963\leq\tilde{x}\leq-13.166$
4	−44.514	$-44.929\leq\tilde{x}\leq-43.979$	−16.849	$-17.170\leq\tilde{x}\leq-16.504$
5	−19.808	$-20.356\leq\tilde{x}\leq-19.434$	–	–
6	−33.318	$-34.502\leq\tilde{x}\leq-31.856$	−19.079	$-19.868\leq\tilde{x}\leq-18.520$
7	−19.270	$-19.875\leq\tilde{x}\leq-18.863$	−13.638	$-13.977\leq\tilde{x}\leq-13.169$
8	−31.625	$-32.022\leq\tilde{x}\leq-31.135$	−32.653	$-33.037\leq\tilde{x}\leq-32.337$
9	−15.074	$-15.460\leq\tilde{x}\leq-14.712$	−14.044	$-14.430\leq\tilde{x}\leq-13.600$
10	−46.146	$-46.707\leq\tilde{x}\leq-45.670$	−35.462	$-36.130\leq\tilde{x}\leq-34.721$
11	−17.914	$-18.562\leq\tilde{x}\leq-17.258$	−15.035	$-15.962\leq\tilde{x}\leq-14.172$
12	−17.758	$-18.172\leq\tilde{x}\leq-17.399$	−14.765	$-15.158\leq\tilde{x}\leq-14.323$
13	−25.465	$-25.848\leq\tilde{x}\leq-25.122$	−19.474	$-19.861\leq\tilde{x}\leq-19.074$
14	−17.590	$-17.951\leq\tilde{x}\leq-17.128$	−17.389	$-17.910\leq\tilde{x}\leq-16.756$
15	−21.449	$-21.766\leq\tilde{x}\leq-21.116$	−16.592	$-17.030\leq\tilde{x}\leq-16.339$
16	−23.931	$-24.237\leq\tilde{x}\leq-23.475$	−12.978	$-13.590\leq\tilde{x}\leq-12.479$
17	−21.019	$-21.508\leq\tilde{x}\leq-20.502$	−21.059	$-21.721\leq\tilde{x}\leq-20.572$
18	−14.685	$-15.163\leq\tilde{x}\leq-13.848$	−14.378	$-14.708\leq\tilde{x}\leq-14.072$
19	−15.000	$-15.335\leq\tilde{x}\leq-14.711$	−15.445	$-15.829\leq\tilde{x}\leq-15.078$
20	−22.789	$-23.466\leq\tilde{x}\leq-22.013$	−17.114	$-17.429\leq\tilde{x}\leq-16.855$
21	−18.306	$-18.808\leq\tilde{x}\leq-17.917$	−17.257	$-17.795\leq\tilde{x}\leq-16.487$
22	−24.755	$-25.309\leq\tilde{x}\leq-24.267$	−17.891	$-18.070\leq\tilde{x}\leq-17.664$

In the first row the numbering of the starting complex is given.

complex indicating weaker host–guest interactions. Energies of interactions are listed in Table 4. In the median test (see Fig. 12) 14 pairs are found showing a significant preference of *R* over *S*. In addition the *R*-enantiomer is able to form nearly twice as many hydrogen bonds as the *S*-enantiomer.

The positive influence of the ethyl substituent in **3R** and **3S** leads to the assumption that this effect should also be observable for the compounds **4R** and **4S** (5-ethyl-3-hydroxy-4-methyl-2[5*H*]-furanone). However, in contrast to the binding properties of **3R** and **3S** the ethyl group at the chiral center of the dihydrofuranones impairs the formation of optimal interaction geometries for enantioselective binding. Despite the tight fixation of the chiral centers of **4R** and **4S** nearby the chiral centers C2 and C3 at the wider opening of the cyclodextrin cavity, there is no increase in enantioselectivity observable (see Fig. 17). This is nicely mirrored in the result of the median test which yielded a preference of *R* over *S* also for 14 pairs (see Fig. 13 and Table 5).

While the chiral separation of the dihydrofuranones **3** and **4** has already been successfully finished the exact attachment of the absolute configurations to the experimentally determined elution order is still in progress. Therefore, the constructed interaction model has been used as a basis for the prediction of the hitherto unknown elution sequences of the compounds **3** and **4**. As a result of the developed statistical evaluation methodology of the described MD simulations, a correlation of the calculated interaction energies with the complex stability of the diastereomeric complexes was made up. For both enantiomeric pairs **3** and **4** the R-complexes seem to be energetically preferred. They are able to form the more stable diastereomeric

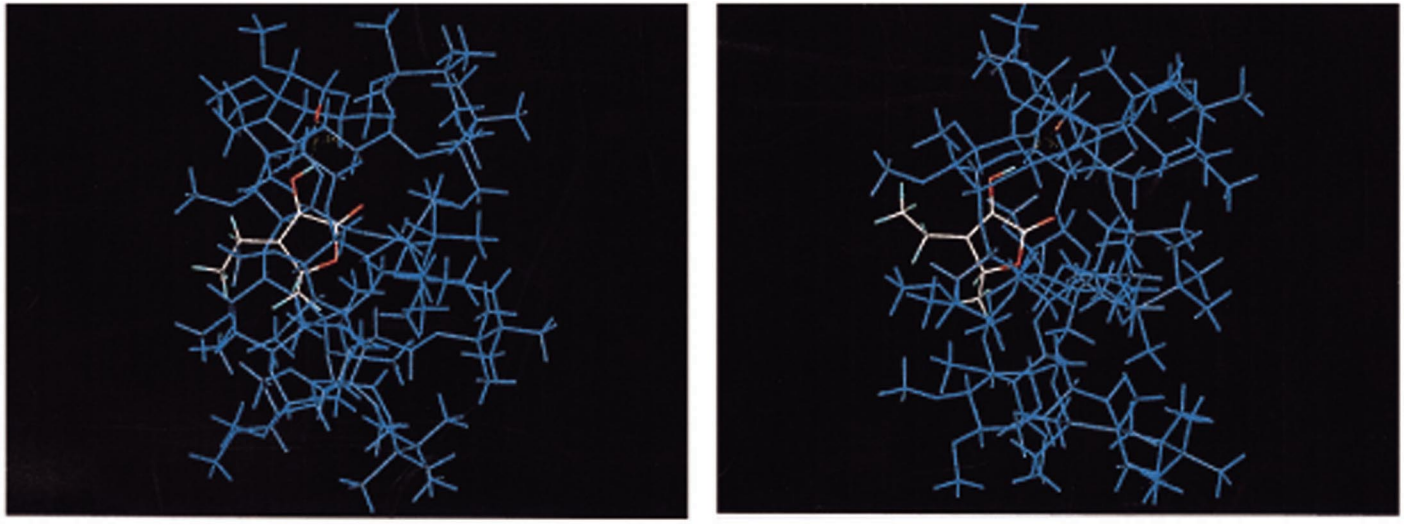

Fig 16.

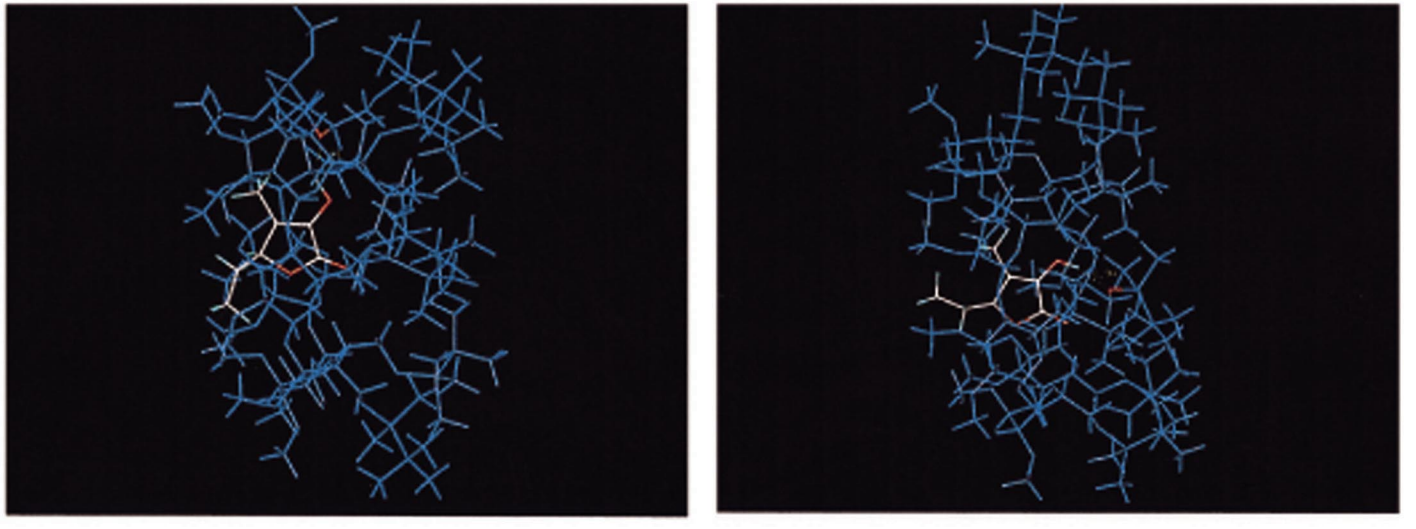

Fig 17.

Fig. 16. One of the favourable complex geometries between **3R** (left side) and **3S** (4-ethyl-3-hydroxy-5-methyl-2[5*H*]-furanone) and heptakis(2,3-di-O-methyl-6-O-*tert*.-butyldimethylsilyl)-β-cyclodextrin. Both complex geometries clearly indicate the contacts of the ethyl group with the chiral centers at the lip of the cavity and the hydrogen bond interactions (dotted lines).

Fig. 17. One of the favourable complex geometries between **4R** (left side) and **4S** (5-ethyl-3-hydroxy-4-methyl-2[5*H*]-furanone) and heptakis(2,3-di-O-methyl-6-O-*tert*.-butyldimethylsilyl)-β-cyclodextrin. Despite the tight fixation of the ligands in the cavity and the possible hydrogen bonds (dotted lines) there is no increase in enantioselectivity observable.

Table 4
Median $\tilde{x}$ of the interaction energy with the confidence interval CI$\tilde{x}$ (α=0.05) of the compounds **3R** and **3S**

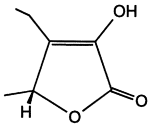

3 R

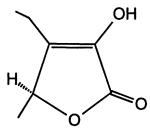

3 S

CD	$\tilde{x}$	CI$\tilde{x}$	$\tilde{x}$	CI$\tilde{x}$
1	−40.883	−41.304≤$\tilde{x}$≤−40.488	−16.740	−17.095≤$\tilde{x}$≤−16.340
2	−16.620	−16.900≤$\tilde{x}$≤−16.323	−13.532	−13.924≤$\tilde{x}$≤−13.124
3	−14.601	−15.000≤$\tilde{x}$≤−14.220	−14.596	−14.780≤$\tilde{x}$≤−14.216
4	−36.049	−37.351≤$\tilde{x}$≤−34.437	−33.399	−34.610≤$\tilde{x}$≤−32.171
5	−18.379	−18.822≤$\tilde{x}$≤−17.996	−17.337	−17.516≤$\tilde{x}$≤−17.016
6	−26.479	−27.260≤$\tilde{x}$≤−25.460	−22.045	−23.347≤$\tilde{x}$≤−20.984
7	−51.034	−51.476≤$\tilde{x}$≤−50.699	−38.669	−39.229≤$\tilde{x}$≤−38.230
8	−34.688	−35.021≤$\tilde{x}$≤−34.386	−30.411	−30.695≤$\tilde{x}$≤−30.030
9	−13.866	−14.075≤$\tilde{x}$≤−13.666	−13.856	−14.196≤$\tilde{x}$≤−13.573
10	−40.515	−40.886≤$\tilde{x}$≤−40.142	−38.717	−39.229≤$\tilde{x}$≤−38.345
11	−15.909	−16.352≤$\tilde{x}$≤−15.552	−16.057	−16.443≤$\tilde{x}$≤−15.677
12	−13.137	−13.443≤$\tilde{x}$≤−12.725	−15.692	−16.181≤$\tilde{x}$≤−15.337
13	−36.874	−37.305≤$\tilde{x}$≤−36.407	−33.801	−34.424≤$\tilde{x}$≤−33.176
14	−42.921	−43.581≤$\tilde{x}$≤−42.351	−41.437	−41.723≤$\tilde{x}$≤−41.122
15	−30.252	−30.593≤$\tilde{x}$≤−29.851	−14.841	−15.248≤$\tilde{x}$≤−14.430
16	−43.586	−43.942≤$\tilde{x}$≤−43.288	−40.016	−40.439≤$\tilde{x}$≤−39.560
17	−44.849	−45.428≤$\tilde{x}$≤−44.506	−35.920	−36.361≤$\tilde{x}$≤−35.490
18	−19.944	−20.453≤$\tilde{x}$≤−19.024	−19.789	−20.130≤$\tilde{x}$≤−19.267
19	−14.257	−15.190≤$\tilde{x}$≤−13.520	−16.191	−16.525≤$\tilde{x}$≤−15.862
20	−40.857	−41.153≤$\tilde{x}$≤−40.562	−38.927	−39.322≤$\tilde{x}$≤−38.555
21	−40.585	−40.940≤$\tilde{x}$≤−40.181	−43.775	−44.084≤$\tilde{x}$≤−43.417
22	−35.970	−36.715≤$\tilde{x}$≤−35.305	−36.273	−36.720≤$\tilde{x}$≤−35.916

In the first row the numbering of the starting complex is given.

complex states resulting in longer retention times in the chromatographic separation process. Therefore the most probable elution order for the enantiomeric pairs is *S* before *R*. Despite the statistical significance of prediction it has to be kept in mind that only a snapshot of the whole separation process is represented by these theoretical simulations.

4. Discussion

The following considerations should shed some light onto the complex chromatographic process and the forces involved in enantiomeric separation. Firstly, the number of hydrogen bonds found in the diastereomeric complexes is in most cases higher for the more retained enantiomer. The distribution pattern of the binding partners involved in hydrogen bond interactions can be used to describe the preferred location of the ligand in the cyclodextrin cavity. The intermediate diastereomeric complexes can be stabilized by the hydrogen bonds fixing the guest molecules in an energetically favorable interaction geometry leading to strong enantioselective interactions. However, the ability to form this kind of interaction is not essential for enantiomeric separation because the chiral discrimination also takes place for the methoxy substituted compounds **2R** and **2S**.

Secondly, to elucidate the contribution of the hydrogen bonds to the interaction energy the total energy can be partitioned into the van der Waals and the electrostatic part. In the CVFF force field hydrogen bonds are represented by the standard van der

Table 5
Median $\tilde{x}$ of the interaction energy with the confidence interval CI$\tilde{x}$ (α=0.05) of the compounds **4R** and **4S**

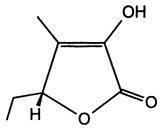

4 R

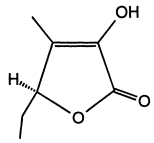

4 S

CD	$\tilde{x}$	CI$\tilde{x}$	$\tilde{x}$	CI$\tilde{x}$
1	−38.014	−38.493≤$\tilde{x}$≤−37.524	−33.945	−34.798≤$\tilde{x}$≤−33.306
2	−17.106	−17.470≤$\tilde{x}$≤−16.746	−14.574	−14.838≤$\tilde{x}$≤−14.265
3	−25.094	−26.312≤$\tilde{x}$≤−24.146	−19.615	−20.128≤$\tilde{x}$≤−19.004
4	−13.084	−13.515≤$\tilde{x}$≤−12.810	−14.121	−14.349≤$\tilde{x}$≤−13.832
5	−17.303	−17.587≤$\tilde{x}$≤−16.907	−17.498	−17.825≤$\tilde{x}$≤−17.078
6	−19.591	−20.085≤$\tilde{x}$≤−19.109	−17.154	−17.626≤$\tilde{x}$≤−16.774
7	−47.593	−47.878≤$\tilde{x}$≤−47.366	−39.368	−39.821≤$\tilde{x}$≤−38.904
8	−37.894	−38.436≤$\tilde{x}$≤−37.492	−39.736	−40.522≤$\tilde{x}$≤−39.121
9	−13.986	−14.310≤$\tilde{x}$≤−13.597	−13.714	−13.976≤$\tilde{x}$≤−13.496
10	−45.040	−45.775≤$\tilde{x}$≤−44.528	−36.394	−39.906≤$\tilde{x}$≤−35.901
11	−15.566	−15.729≤$\tilde{x}$≤−15.291	−13.645	−14.043≤$\tilde{x}$≤−13.294
12	−22.798	−23.164≤$\tilde{x}$≤−22.390	−11.185	−11.583≤$\tilde{x}$≤−10.936
13	−42.295	−42.836≤$\tilde{x}$≤−41.868	−37.613	−37.866≤$\tilde{x}$≤−37.367
14	−44.953	−45.253≤$\tilde{x}$≤−44.701	−47.879	−48.394≤$\tilde{x}$≤−47.599
15	−17.372	−17.782≤$\tilde{x}$≤−16.929	−19.128	−19.614≤$\tilde{x}$≤−18.605
16	−35.289	−35.602≤$\tilde{x}$≤−34.878	−34.474	−34.854≤$\tilde{x}$≤−34.198
17	−14.471	−14.739≤$\tilde{x}$≤−14.175	−15.978	−16.397≤$\tilde{x}$≤−15.636
18	−11.171	−11.659≤$\tilde{x}$≤−10.750	−13.457	−13.874≤$\tilde{x}$≤−13.227
19	−18.184	−18.501≤$\tilde{x}$≤−17.952	−13.372	−13.757≤$\tilde{x}$≤−12.956
20	−41.566	−41.896≤$\tilde{x}$≤−41.290	−43.357	−43.630≤$\tilde{x}$≤−42.955
21	−13.683	−14.117≤$\tilde{x}$≤−13.151	−12.683	−13.006≤$\tilde{x}$≤−12.358
22	−41.578	−41.934≤$\tilde{x}$≤−41.111	−16.603	−17.101≤$\tilde{x}$≤−16.334

In the first row the numbering of the starting complex is given.

Waals and electrostatic parameters. As a special hydrogen bond interaction function is not included in the force field terms it has been shown that the energy profit of a hydrogen bond is sufficiently reflected by the increase in electrostatic energy [64–66]. The possibility to form hydrogen bonds therefore to a higher amount of the electrostatic part in the total interaction energy. As a consequence the electrostatic interaction energy for the compounds **2R** and **2S** is lower than for the hydroxyl substituted compounds **1**, **3** and **4** (see also Fig. 18). The decrease in enantioselectivity for **2R** and **2S** is congruent with the idea that enantioselectivity is affected by the electrostatic interactions between the cyclodextrin and the guest molecules, and the van

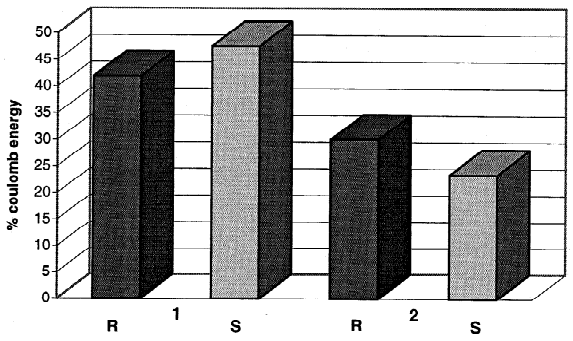

Fig. 18. Comparison of the electrostatic contributions to the total interaction energies for compounds **1R** and **1S** and their methoxy analogues **2R** and **2S**. The possibility to form hydrogen bonds leads to higher electrostatic interactions for the dihydrofuranones **1R/S** in comparison to the methoxy substituted congeners.

der Waals forces are mainly responsible for complex formation [67].

Thirdly, in contrast to the native cyclodextrins the substitution pattern of the heptakis(2,3-di-O-methyl-6-O-*tert*.-butyldimethylsilyl)-β-cyclodextrin does not allow the formation of intramolecular hydrogen bonds. The loss of this property leads to a higher flexibility of the macrocycle as already shown in the conformational analysis of the host molecule. This flexibility plays an important role in the enantioselective binding process. The induced-fit mechanism enables the formation of optimal host–guest geometries. This seems to be of special importance for the chiral recognition because a reduction in conformational flexibility of the cyclodextrin leads to a drastic decrease in enantioselectivity.

The inclusion of the guest molecules into the cavity is of major importance for the chiral separation process. The heptakis(2,3-di-O-methyl-6-O-*tert*.-butyldimethylsilyl)-β-cyclodextrin reveals higher enantioselectivity than its α- and γ-homologues [61,68]. For a number of compounds the cavity of the α-cyclodextrin is too small for complete inclusion while in γ-cyclodextrins tight binding only for sterically more demanding ligands has been observed. The heptakis(2,3-di-O-methyl-6-O-*tert*.-butyldimethylsilyl)-β-cyclodextrin however is able to form stable inclusion complexes with a wide range of guest molecules. The evidence for the inclusion mechanism in enantioselective binding is supported by the observation that small modifications in the substitution pattern of the ligands can lead to a decrease in enantioselectivity as a consequence of sterical hindrance during the penetration into the cavity.

From our observations some useful hints can be deduced and enable us to propose prerequisites for enantioselective binding in cyclodextrins. For the chiral discrimination process using heptakis(2,3-di-O-methyl-6-O-*tert*.-butyldimethylsilyl)-β-cyclodextrin the inclusion property of the host molecule is essential. Enantioselective binding is only possible by complete or at least partial inclusion of the ligand into the cavity. Contacts at the outer surface of the cyclodextrin are possible but do not contribute to chiral discrimination.

Hydrogen bonds are able to stabilize the host–guest geometries and bring the ligands into the situation to form enough chiral contacts to the cyclodextrin resulting in tight enantioselective binding. The intermolecular forces in the host–guest complexes have to be strong enough to enable a sufficient number of chiral interactions. The flexibility of the heptakis(2,3-di-O-methyl-6-O-*tert*.-butyldimethylsilyl)-β-cyclodextrin offers the possibility to form energetically favorable interaction geometries.

5. Conclusion

The presented methodology for the construction of the interaction model used in this study is capable of simulating the experimental data. Comprehensive MD simulations yielded a realistic picture of the conformational flexibility and the enantioselective binding properties of the host–guest complexes. Only by means of these MD calculations the time dependent motional behavior of the system and the multiple contacts between the guest and the host molecules can be simulated. This is congruent with the results of a recently published theoretical study dealing also with the enantiomeric binding of ligands to modified cyclodextrins during gas chromatographic separation [69].

The results provide an interesting insight into the possible nature of interactions between the dihydrofuranones and the cyclodextrin host. The inclusion mechanism seems to be of special importance for chiral recognition. The resulting intermediate diastereomeric complex geometries can be stabilized by hydrogen bonds. The proposed induced-fit mechanism is an essential contribution for enantioselective binding between selector and selectand. The presented model may serve as a basis for the prediction of hitherto unknown elution sequences at modified cyclodextrins and may be used as a helpful tool in the design of new cyclodextrin based separation columns. However, the general applicability of the procedure described in this work still has to be proven. The only way to establish that the methodology is a sound approach, is to reproduce correctly the retention orders of many separations carried out experimentally. This work is in progress in our laboratory.

Acknowledgements

Thank is due, for the financial support of this work, to the Fonds der Chemischen Industrie.

References

[1] R.M.A. Knegtel, B. Strokopytov, D. Penninga, O.G. Faber, H.J. Rozeboom, K.H. Kalk, L. Dijkhuizen, B.W. Dijkstra, J. Biol. Chem. 270 (1995) 29256.
[2] B. Strokopytov, D. Penninga, H.J. Rozeboom, K.H. Kalk, L. Dijkhuizen, B.W. Dijkstra, Biochemistry 34 (1995) 2234.
[3] K.-H. Frömming, Dtsch. Aopth. Ztg. 127 (1987) 2040.
[4] A. Preiss, W. Mehnert, K.-H. Frömming, Pharmazie 50 (1995) 121.
[5] F. Djedaini-Pilard, B. Perly, S. Dupas, M. Miocque, H. Galons, Tetrahedron Lett. 34 (1993) 1145.
[6] J. Szejtli, E. Bolla-Pusztai, P. Szabo, T. Ferenczy, Pharmazie 35(H12) (1980) 779.
[7] M. Thoß, L. Schwabe, K.-H. Frömming, Pharmazie 49 (1994) 252.
[8] R. Reinhardt, W. Engewald, U. Himmelreich, B. Christian, B. Koppenhoefer, J. Chromatogr. Sci. 33 (1995) 236.
[9] V. Schurig, H.-P. Nowotny, D. Schmalzing, Angew. Chem. 101 (1989) 785.
[10] I.H. Hardt, C. Wolf, B. Gehrcke, D.H. Hochmuth, B. Pfaffenberger, H. Hühnerfuss, W.A. König, J. High Resolut. Chromatogr. 17 (1994) 859.
[11] A. Mosandl, J. Chromatogr. 624 (1992) 267.
[12] A. Mosandl, Kontakte (Darmstadt) 3 (1992) 38.
[13] V. Schurig, H.-P. Nowotny, Angew. Chem. 102 (1990) 969.
[14] A. Steinborn, R. Reinhardt, W. Engewald, K. Wyssuwa, K. Schulze, J. Chromatogr. A 697 (1995) 485.
[15] R. Reinhardt, A. Steinborn, K. Anhalt, K. Schulze, J. Chromatogr. A 697 (1995) 475.
[16] K. Jaques, W.M. Buda, A. Venema, P. Sandra, J. Chromatogr. A 666 (1994) 131.
[17] A. Kaunzinger, F. Podebrad, R. Liske, B. Maas, A. Dietrich, A. Mosandl, J. High Resolut. Chromatogr. 18 (1995) 49.
[18] A. Dietrich, B. Maas, A. Mosandl, J. High Resolut. Chromatogr. 18 (1995) 152.
[19] G. Bruche, A. Dietrich, A. Mosandl, J. High Resolut. Chromatogr. 16 (1993) 101.
[20] BIOSYM Technologies Inc., San Diego, CA, USA.
[21] M.J. Frisch, G.W. Trucks, M. Head-Gordon, P.M.W. Gill, M.W. Wong, J.B. Foresman, B.G. Johnson, H.B. Schlegel, M.A. Robb, E.S. Replogle, R. Gomperts, J.L. Andres, K. Raghavachari, J.S. Binkley, C. Gonzales, R.L. Martin, D.J. Fox, D.J. De Frees, J. Baker, J.J.P. Stewart, J.A. Pople, GAUSSIAN 92, Revision C, Gaussian Inc., Pittsburgh, PA, 1992.
[22] I. Tvaroska, T. Bléha, Adv. Carbohydr. Chem. Biochem. 47 (1989) 45.
[23] U. Burkert, N.L. Allinger, Molecular Mechanics, ACS Monograph 177, American Chemical Society, Washington DC, USA, 1982.
[24] J.L. Asensio, M. Martin-Pastor, J. Jimenez-Barbero, Int. J. Biol. Macromol. 17 (1995) 137.
[25] G.A. Jeffrey, R.K. McMullan, S. Takagi, Acta Crystallogr. B 33 (1977) 728.
[26] C. Betzel, W. Saenger, B.E. Hingerty, G.M. Brown, J. Am. Chem. Soc. 106 (1984) 7545.
[27] F.H. Allen, J.E. Davies, J.J. Galloy, O. Johnson, O. Kennard, C.F. Macrae, E.M. Mitchell, J.M. Smith, D.G. Watson, J. Chem. Inf. Comput. Sci. 31 (1991) 187.
[28] S.R. Wilson, W. Cui, Biopolymers 29 (1990) 225.
[29] T. Huber, A.E. Torda, W.F. van Gunsteren, J. Comput.-Aided Mol. Design 8 (1994) 695.
[30] J.M. Salvino, P.R. Seoane, R.E. Dolle, J. Comput. Chem. 14 (1993) 438.
[31] S.R. Wilson, W. Cui, J.W. Moskowitz, K.E. Schmidt, Tetrahedron Lett. 29 (1988) 4376.
[32] J.P. Ryckaert, G. Ciccotti, H.J.C. Berendsen, J. Comput. Phys. 23 (1977) 327.
[33] V. Zabel, W. Saenger, S.A. Mason, J. Am. Chem. Soc. 108 (1986) 3664.
[34] T. Steiner, S.A. Mason, W. Saenger, J. Am. Chem. Soc. 112 (1990) 6184.
[35] T. Steiner, S.A. Mason, W. Saenger, J. Am. Chem. Soc. 113 (1991) 5676.
[36] T. Steiner, W. Saenger, Carbohydr. Res. 259 (1994) 1.
[37] SPARTAN, Wavefunction Inc., Irvine, CA, USA.
[38] M.J.S. Dewar, E.G. Zoebisch, E.F. Healy, J.J.P. Stewart, J. Am. Chem. Soc. 107 (1985) 3902.
[39] J.J.P. Stewart, In: K.B. Lipkowitz, D.B. Boyd (Eds.), Reviews in Computational Chemistry, Vol. 1., VCH, New York, 1990, p. 45.
[40] J.J.P. Stewart, J. Comput. Chem. 10 (1989) 209.
[41] J.J.P. Stewart, J. Comput. Chem. 10 (1989) 221.
[42] S.R. Cox, D.E. Williams, J. Comput. Chem. 2 (1981) 304.
[43] L.E. Chirlian, M.M. Francl, J. Comput. Chem. 6 (1987) 894.
[44] GRID, Version 11, Molecular Discovery Ltd., Oxford, England.
[45] N. Koen de Vries, B. Coussens, R.J. Meier, J. High Resolut. Chromatogr. 15 (1992) 499.
[46] J.E.H. Koehler, M. Hohla, M. Richters, W.A. König, Angew. Chem. 104 (1992) 362.
[47] J.E.H. Koehler, M. Hohla, M. Richters, W.A. König, Chem. Ber. 127 (1994) 119.
[48] F. Kobor, K. Angermund, G. Schomburg, J. High Res. Chromatogr. 16 (1993) 299.
[49] F. Nishioka, I. Nakanishi, T. Fujiwara, K. Tomita, J. Inclusion Phenom. 2 (1984) 701.
[50] K. Harata, K. Uekama, M. Otagiri, F. Hiragayama, Bull. Chem. Soc. Jpn. 56 (1983) 1732.
[51] K. Harata, K. Uekama, M. Otagiri, F. Hiragayama, Y. Ohtani, Bull. Chem. Soc. Jpn. 58 (1985) 1234.
[52] K. Harata, Bull. Chem. Soc. Jpn. 52 (1979) 2451.
[53] W. Saenger, K. Beyer, P.C. Manor, Acta Crystallogr. B 32 (1976) 120.

[54] A. Ganza-Gonzalez, J.L. Vila-Jato, S. Anguiano-Igea, F.J. Otero-Espinar, J. Blanco-Méndez, Int. J. Pharm. 106 (1994) 179.
[55] B. Casu, M. Reggiani, G.R. Sanderson, Carbohydr. Res. 76 (1979) 59.
[56] D. Fercej-Temeljotov, M. Kmet, D. Kocjan, S. Kotnik, A. Resman, U. Urleb, K. Verhnjak, I. Zver, J. Zmitek, Chirality 5 (1993) 288.
[57] K.B. Lipkowitz, S. Raghothama, J. Yang, J. Am. Chem. Soc. 114 (1992) 1554.
[58] D.W. Armstrong, T.J. Ward, R.D. Armstrong, T.E. Beesley, Science 232 (1986) 1132.
[59] W.A. König, Kontakte (Darmstadt) 2 (1990) 3.
[60] H.-G. Schmarr, A. Mosandl, H.-P. Neukom, K. Grob, J. High Resolut. Chromatogr. 14 (1991) 207.
[61] F. Kobor, G. Schomburg, J. High Resolut. Chromatogr. 16 (1993) 693.
[62] A. Dietrich, B. Maas, G. Brand, V. Karl, A. Kaunzinger, A. Mosandl, J. High Resolut. Chromatogr. 15 (1992) 769.
[63] A. Dietrich, B. Maas, A. Mosandl, J. Microcolumn Sep. 6 (1994) 33.
[64] S. Lifson, A.T. Hagler, P. Dauber, J. Am. Chem. Soc. 101 (1979) 5111.
[65] A.T. Hagler, S. Lifson, P. Dauber, J. Am. Chem. Soc. 101 (1979) 5122.
[66] A.T. Hagler, P. Dauber, S. Lifson, J. Am. Chem. Soc. 101 (1979) 5131.
[67] K.B. Lipkowitz, K.M. Green, J.-A. Yang, G. Pearl, M.A. Peterson, Chirality 5 (1993) 51.
[68] K. Cabrera, G. Schwinn, Kontakte (Darmstadt) 3 (1989) 3.
[69] K.B. Lipkowitz, G. Pearl, B. Coner, M.A. Peterson, J. Am. Chem. Soc. 119 (1997) 600.